Quantum Electronics **49** (4) 337–343 (2019)

https://doi.org/10.1070/QEL16971

Nonlinear interferometer for increasing the contrast ratio of intense laser pulses

E.A. Khazanov, S.Yu. Mironov

Abstract. **The possibility is shown for increasing the contrast ratio of intense (TW cm^{-2}) femtosecond laser pulses by using a nonlinear Mach–Zehnder interferometer, and also under the conditions of cascade quadratic nonlinearity in two tandem uniaxial crystals detuned from the matching direction to opposite sides. In both the cases, the peak intensity slightly falls (by ~10%) and with additional chirp mirrors may even exceed the initial intensity.**

Keywords: *nonlinear Mach–Zehnder interferometer, terawatt laser pulses, contrast ratio.*

1. Introduction

The peak power and time-domain contrast of ultrahigh-power laser pulses are the key parameters in investigations of substance behaviour in extremely ultraintense light fields and in generation of charged particle bunches. Hereinafter, under the contrast ratio (or contrast) is meant the ratio of a pulse peak intensity to that in the pulse tails. A high contrast prevents target destruction prior to the main pulse arrival, whereas a higher peak intensity of laser pulses focused onto a target will help solve formerly inaccessible experimental problems related to investigations of vacuum nonlinearity, electron–positron pair generation, etc. Note that presently the record peak intensity reached in experiments is 10^{22} W cm^{-2} [1]. Further increase may be realised by improving the beam focusing quality, increasing the pulse energy, and/or shortening pulse duration [2–6]. In addition, presently, further time compression is experimentally demonstrated for terawatt-level femtosecond laser pulses with self-phase modulation and chirped mirrors [4, 6, 7]. Several successive stages of time compression will finally yield petawatt-power laser pulses with a duration of several periods of light field oscillations [5], which has not been realised experimentally yet.

The profile of a laser pulse is conventionally divided to the sections of far and near contrast. These sections are separated by a 1-ps boundary from the main maximum. The near contrast depends on the matching of the stretcher–compressor pair, whereas the far contrast is affected by the methods of pulse amplification employed. The required level of the far contrast is determined by the peak intensity and threshold of plasma generation. The contrast is conventionally increased by using the devices in which the transmission (or reflection) coefficient for a laser radiation depends on the intensity. For improving the pulse time profile, plasma mirrors [8–10], cross-polarised wave (XPW) generation [11–13], second harmonic generation [2, 14–16], and other methods are currently used. Plasma mirrors and (or) second harmonic generation can be directly applied for obtaining petawatt laser pulses. The XPW method is conventionally used in input stages of petawatt laser systems [13]. This is mainly explained by the lack of large-aperture crystals (more than 10 cm) and a low conversion efficiency (~30% in energy) [11, 13, 17]. Note than XPWs are generated by using nonlinear crystals with an anisotropic tensor of cubic nonlinearity (such as CaF_2 and BaF_2). A nonlinear-optical process of XPW generation broadens the spectrum of intense laser pulses and introduces the frequency modulation of phase, which can be compensated for due to reflection from chirped mirror surfaces. This can preserve and even increase the peak pulse power with a better contrast.

In the present work we analyse the possibility of using two methods for increasing the contrast ratio of superpower laser pulses. The first method is based on Kerr nonlinearity in transmitting elements of a Mach–Zehnder interferometer. Note that the employment of a Mach–Zehnder interferometer for producing the optical shutter in which the transmission coefficient depends on radiation intensity was earlier considered in [18–20]. The second method implies the employment of cascade nonlinearity in two tandem uniaxial crystals detuned from the matched position to opposite sides similarly to [21].

2. Employment of a nonlinear Mach–Zehnder interferometer for increasing the contrast of ultrahigh-power laser pulses

Double-beam Mach–Zehnder interferometers are widely used in precise measurements of the phase inhomogeneities acquired by a laser beam in one of its channels. A schematic of such an interferometer is shown in Fig. 1. The interferometer comprises two splitting plates (*1*), which are transmitting optical elements, and two mirrors (*2*). An interferometer of this kind can also be used for increasing the contrast ratio [22].

Possibilities of increasing the contrast of intense (with a power density of several TW cm^{-2}) laser pulses by using a Mach–Zehnder interferometer can be demonstrated with a simplest mathematical model. Assume that transmission elements (*1*) are similar and have the transmission and reflection coefficients, respectively, T and R satisfying the relationship $R + T = 1$. We will also assume that mirrors (*2*) introduce no losses and do not modulate the spectral phase of a

E.A. Khazanov, S.Yu. Mironov Institute of Applied Physics, Russian Academy of Sciences, ul. Ul'yanova 46, 603950 Nizhny Novgorod, Russia; e-mail: khazanov@appl.sci-nnov.ru

Received 19 February 2019
Kvantovaya Elektronika **49** (4) 337–343 (2019)
Translated by N.A. Raspopov

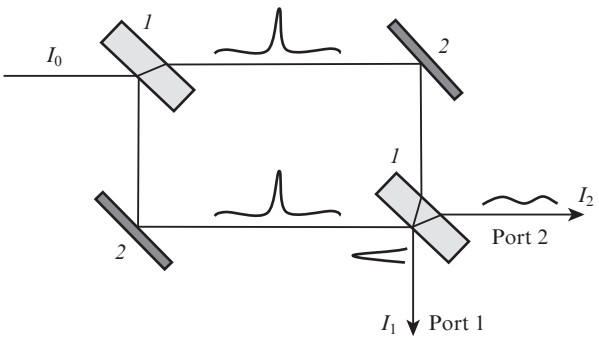

Figure 1. Schematic of a Mach–Zehnder interferometer: (*1*) transmitting optical elements; (*2*) mirrors; I_0 is the initial intensity; I_1 and I_2 are the intensities at interferometer outputs for ports 1 and 2, respectively.

pulse, and that the splitting plates are ideal without parasitic reflections from rear faces. Note that it is not always possible to completely exclude parasitic reflections in experiments. In those cases, reflected in this way pre-pulses or amplified spontaneous luminescence may interact with each other at the interferometer output. This effect can be reduced if rear faces of the splitting plates are arranged at the Brewster angle. For example, splitting plates from fused silica with reflection at the Brewster angle may reduce the intensity of a homogeneous wide-band radiation with a bandwidth of 0.2ω ($\omega = 2.07\times10^{15}$ s^{-1} is the carrying frequency corresponding to the wavelength of 910 nm) by a factor of approximately 10^7. In the frameworks of this approximation, the expressions for intensities I_1 and I_2 at outputs of the arms (ports) have the form:

$$I_1(t) = \frac{c}{8\pi}|A_1|^2 = \{1 - 2(1-R)R + 2(1-R)R\cos[\Delta\varphi_L + 2(1-R)B(t)]\}I_0(t),$$
$$I_2(t) = \frac{c}{8\pi}|A_2|^2 = \{2(1-R)R - 2(1-R)R\cos[\Delta\varphi_L + 2(1-R)B(t)]\}I_0(t). \quad (1)$$

Here, I_0 is the intensity at the interferometer input ($I_0 = I_1 + I_2$); $\Delta\varphi_L$ is the linear phase difference which pulses acquire while propagating along the interferometer arms; $B(t) = (2\pi/\lambda)I_0(t)\gamma h$ is the nonlinear phase (B-integral); h is the optical thickness of the splitting plates; λ is the wavelength; and γ is the cubic nonlinearity factor. Note that this model does not take into account the influence of group velocity dispersion on the laser pulses passed through the beam splitters, because the interferometer is assumed to operate in the conditions where the dispersion length L_d [$L_d = \tau^2/k_2$, where τ is the duration and k_2 is the parameter of group velocity dispersion (in fs mm^{-1})] substantially exceeds the optical thickness of the beam splitters and the characteristic spatial scale L_b, in which $B(0) = 1$. For example, for the plates from fused silica and radiation of duration 50 fs with the centre wavelength of 910 nm and intensity of 1 TW cm^{-2} we have $L_d = 86$ mm, whereas $h = \pi L_b = 1.9$ mm.

In the linear case ($B = 0$), the value of I_1 in (1) may be exactly zero at $\Delta\varphi_L = \pi$ and $R = 0.5$. At elevated intensity, cubic nonlinearity effects become substantial; the pulses accumulate a nonlinear phase and the phase balance breaks. In the result, the dark port of the interferometer becomes bright at $B(0) = \pi$. Note that the strongest phase mismatch is observed only for a central part of the pulse and is actually absent in the tails. In the pulse tails, the interferometer remains closed. Obviously, in the conditions $\Delta\varphi = \pi$, $R = 0.5$, and $B(0) = \pi$, intensity I_1 takes a maximal value. For this case, profiles of the initial pulse of duration 50 fs with the far contrast level of 10^{-7} are presented in Fig. 2 along with the pulses at the output of port 1.

According to Fig. 2, the far contrast of the pulse increases from 10^{-7} to 10^{-20}, its duration shortens from 50 fs to 38 fs, and the peak intensity remains the same $I_1(0) = I_0(0)$. Note that an intense laser pulse propagating in transmitting optical elements broadens its spectrum and its phase acquires a frequency modulation. The employment of chirped mirrors similarly to the method described in [2–6] makes it possible to additionally reduce the pulse duration to 24 fs and increase the intensity by a factor of 1.56 as compared to the initial value. A profile of the pulse with an enhanced

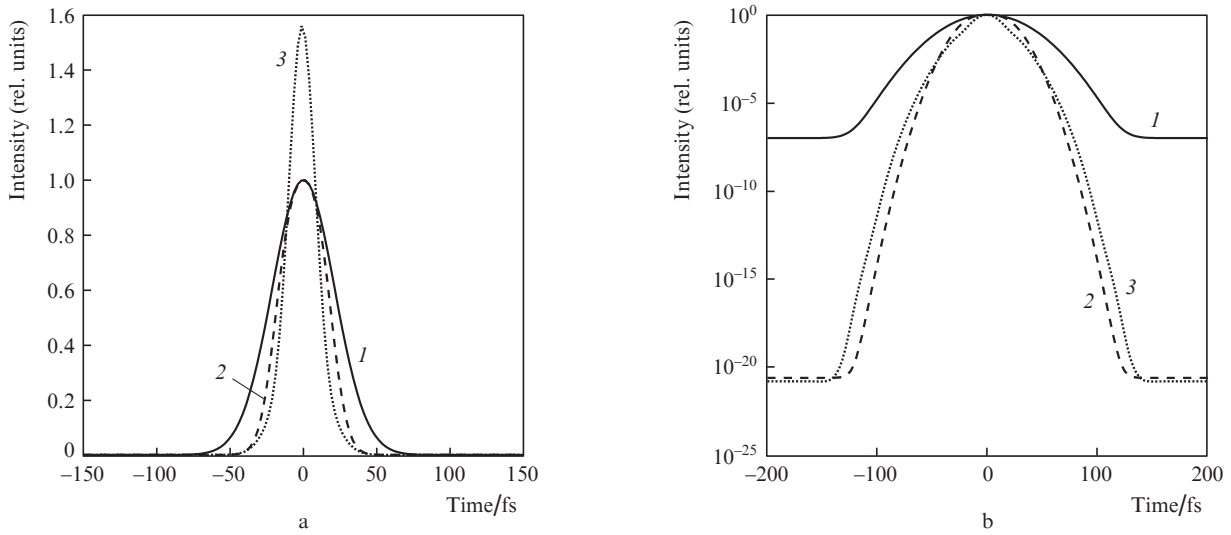

Figure 2. Enhancement of the contrast by using a Mach–Zehnder interferometer. Intensity distributions of the following pulses are shown: (*1*) initial, (*2*) at the output of port 1 of the interferometer, and (*3*) after the additional time compression with chirp mirrors in the (a) linear and (b) logarithmic scales.

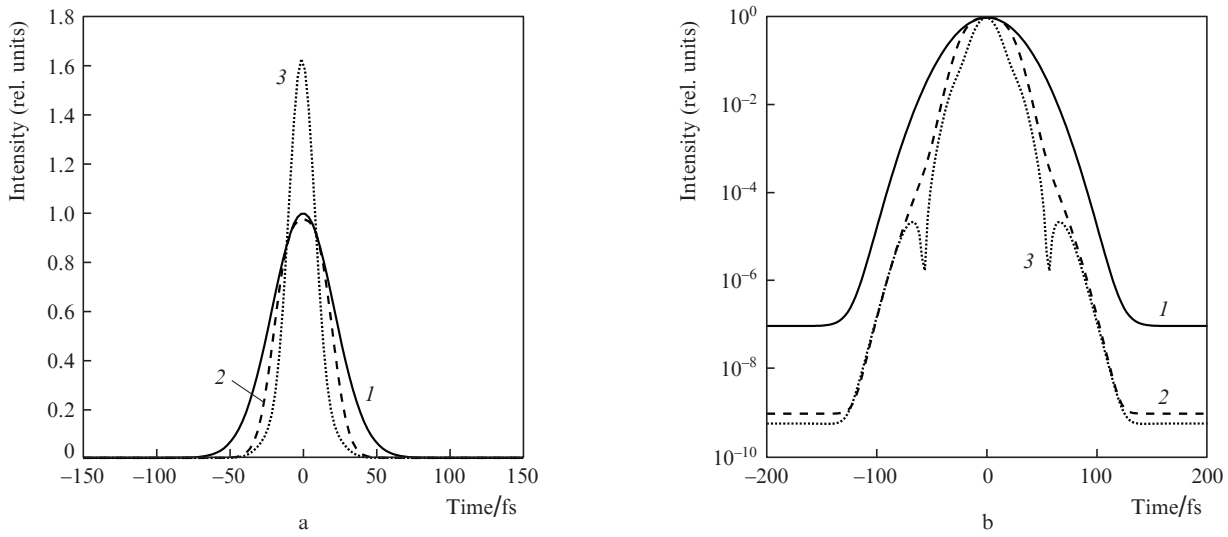

Figure 3. The same as in Fig. 2 at $B(0) = \pi$, $\Delta\varphi_L = \pi$ and $R = 0.45$.

contrast after reflection from the chirped mirrors is shown in Fig. 2 [curve (*3*)].

Let us now analyse how the interferometer operation is affected by imperfectly produced splitting plates [R is distinct from 0.5 (Fig. 3) and the optical thickness is not homogeneous (Fig. 4)] and by intensity instability from pulse to pulse [violated condition $B(0) = \pi$ (Fig. 5)].

According to formulas (1), a distinction of reflection coefficient R from 0.5 results in inessential reduction of the peak intensity for a pulse with improved contrast. At $R = 0.45$, the peak intensity falls by 3% only. However, this distinction affects the value of the far contrast more noticeably (Fig. 3). Note that correction of the spectrum phase with chirped mirrors makes it possible to shorten the pulse duration and increase its intensity by a factor of approximately 1.6 as compared to the initial value (see Fig. 3a).

The far contrast is mostly affected by the linear phase mismatch which arises due to imperfect surfaces of mirrors or beam splitters. In this case, the expression $\Delta\varphi_L$ in (1) takes the form: $\Delta\varphi_L = (2\pi/\lambda)(n-1)\Delta$, where Δ is the random value with a root-mean-square deviation $\Delta\Lambda$ and n is the refraction index of a plate or mirror substrate. Time profiles of the initial pulse and pulses with improved time-domain contrast at $\Delta\varphi_L = \pi$ and $\Delta\Lambda = \lambda/[10(n-1)]$ are shown in Fig. 4 for the case $R = 0.5$ and $B(0) = \pi$ in the linear and logarithmic scales. The path difference error $\Delta\Lambda = \lambda/[10(n-1)]$ substantially worsens the contrast (see Fig. 4b). Thereby, the accuracy of surface fabrication of mirrors and beam splitters used in the interferometer should be substantially better than $\lambda/[10(n-1)]$.

Fluctuations of the peak intensity at the interferometer input change the pulse parameters at output from an opened port. The peak intensity in this case insignificantly falls. For example, a reduction (increase) in the intensity by 20% at $R = 0.5$ and $\Delta\varphi_L = \pi$ reduces the peak intensity by only 10% (Fig. 5a) and a variation of the peak intensity does not affect the level of the far contrast (Fig. 5b).

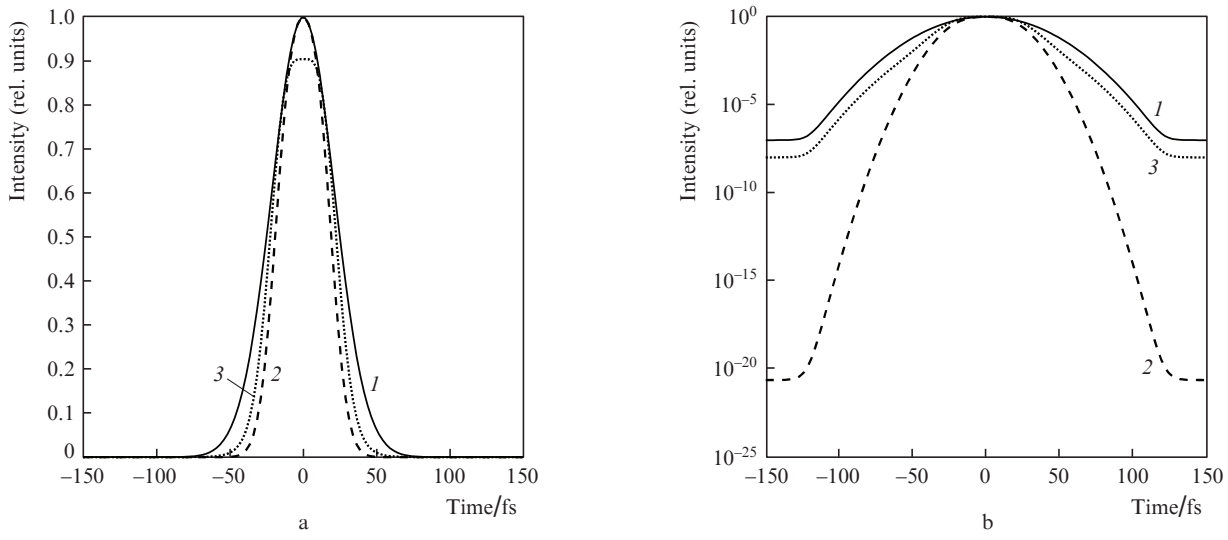

Figure 4. Profiles of (*1*) laser pulses at interferometer input and of (*2*,*3*) pulses with improved contrast at (*2*) $R = 0.5$, $\Delta\varphi_L = \pi$, $B(0) = \pi$ and (*3*) $R = 0.5$, $\Delta\varphi_L = \pi$, $B(0) = 0.8\pi$ in the (a) linear and (b) logarithmic scales.

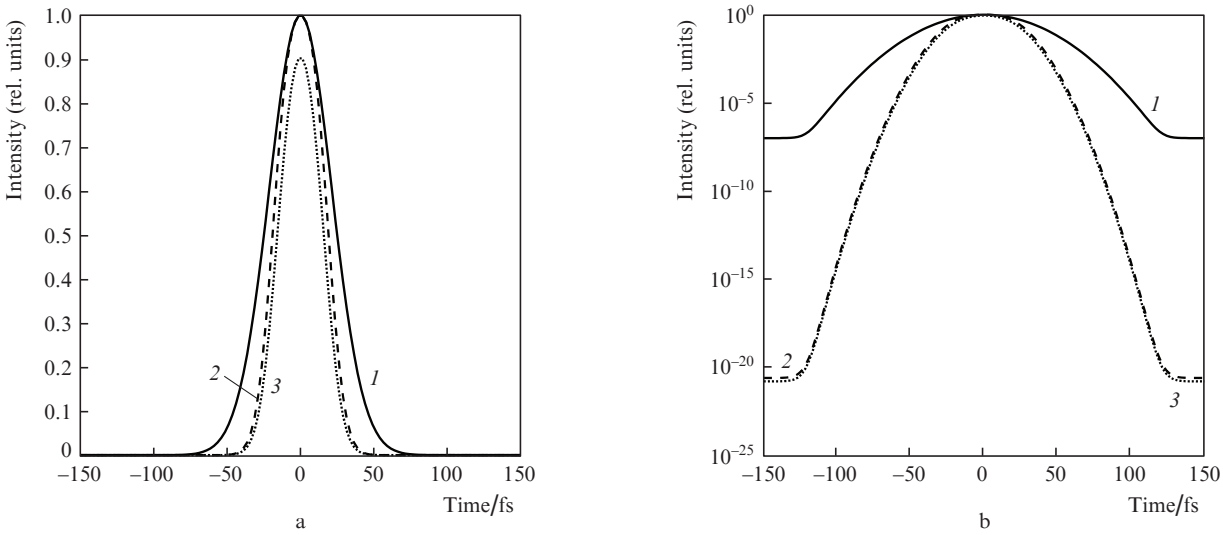

Figure 5. Profiles of (*1*) the initial pulse and of (*2*, *3*) pulses with improved contrast at (*2*) $R = 0.5$, $B(0) = \pi$, $\Delta\varphi_L = \pi$ and (*3*) $R = 0.5$, $B(0) = \pi$, $\Delta\varphi_L = \pi + 2\pi/10$ in the (a) linear and (b) logarithmic scales.

Under varied interferometer parameters, the profile of a pulse with an enhanced contrast most strongly depends on the linear effects: the beam path difference and distinction of the beam splitter reflection coefficient R from 0.5.

3. Increase in the contrast by using cascade second harmonic generation

3.1. Idea of the method

It is known [20, 23, 24] that detuning from the phase matching direction in the process of frequency doubling results in an effective addition to the refraction index, which linearly depends on the intensity and has the sign determined by that of the mismatch between the wave vectors of the interacting first and second harmonic waves Δk. It is commonly supposed that this addition is related to manifestation of the cascade quadratic nonlinearity [23]. Control of the sign of the wave vector mismatch by varying the propagation direction of the fundamental wave in a frequency-doubling crystal makes it possible to monitor the contribution of Kerr nonlinearity and the efficiency of accompanying effects [25, 26]. Physically, the addition to the reflection index is related with the fact that if there is deviation from the phase matching direction, the phase velocities for the fundamental and second-harmonic waves differ from each other and the energy is backward re-pumped in the process of conversion to second harmonic. Photons generated from the second-harmonic wave have a phase velocity distinct from that of initial photons of the fundamental wave, which explains the phase shift. This effect may be used for fabricating optical devices with an intensity-dependent absorption coefficient [21].

Consider the problem on a possible increase in the time-domain contrast by using the optical scheme, which comprises two tandem uniaxial crystals with the orthogonal matching planes (these are also called interaction critical planes) and a polariser (Fig. 6). A laser pulse linearly polarised in the plane xy (at an angle of 45° with respect to yz plane) is sequentially directed to crystal 1 and then to crystal 2. The polariser is adjusted in such a way that at low intensity (when quadratic and cubic polarisation effects are not essential) the output radiation completely passes through the polariser. For increasing

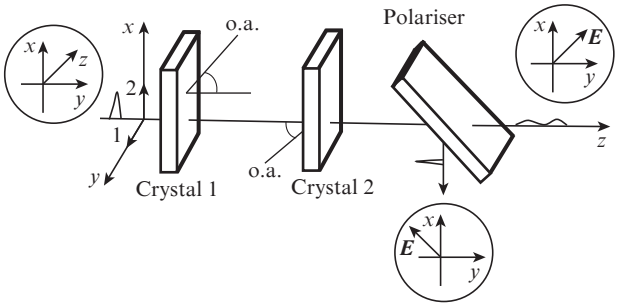

Figure 6. Schematic of contrast enhancement with two tandem uniaxial crystals; o.a. is the optical axis.

contrast, both the crystals should be detuned from the phase matching directions in opposite sides: for the first crystal in the xz plane and for the second crystal in the yz plane. The efficiency of second harmonic generation (we limit ourselves by the oo-e synchronism) in both the crystals should be negligible. In the first crystal, the fundamental wave polarised along the y axis participates in frequency doubling and in the second crystal it does the fundamental wave polarised along the x axis (see Fig. 6). The fundamental and second-harmonic waves undergo self- and cross-interaction effects due to manifestation of the frequency dispersion of the linear part of the refraction index.

If crystal thicknesses and their angular detuning from the phase-matching direction are properly chosen, one can make the phase difference arisen due to quadratic and cubic nonlinearity close to π at the output from the second crystal for the orthogonal components of the fundamental wave. The phase difference related to nonlinearities arises only at a sufficiently high pulse intensity, that is, near the maximum. In this region, the polarisation turns by 90° relative to the initial polarisation. In the result, by using a polariser one can select this region and increase the contrast.

The problem of contrast enhancement with the employment of two uniaxial crystals and a polariser can be stated as follows: at a prescribed pulse intensity, it is necessary to find the crystal thicknesses and the angles of detuning from the

phase matching direction that would provide the maximal peak intensity for the pulse reflected from the polariser with an enhanced contrast.

3.2. Employment of the method as applied to intense femtosecond laser pulses

In the quasi-optical approximation, modification of the pulse parameters of the fundamental and second-harmonic waves in crystal 1 in the case of oo-e interaction can be described by the system of equations:

$$\begin{aligned}
&\frac{\partial A_1}{\partial z} - \mathrm{i}\frac{k_{21}}{2}\frac{\partial^2 A_1}{\partial \eta^2} = -\mathrm{i}\beta A_3 A_1^* e^{-\mathrm{i}\Delta kz} \\
&\quad - \mathrm{i}A_1 \sum_{j=1}^{3} \gamma_{1,j} |A_j|^2, \\
&\frac{\partial A_2}{\partial z} + \left(\frac{1}{u_2} - \frac{1}{u_1}\right)\frac{\partial A_2}{\partial \eta} - \mathrm{i}\frac{k_{22}}{2}\frac{\partial^2 A_2}{\partial \eta^2} = -\mathrm{i}A_2 \sum_{j=1}^{3} \gamma_{2,j} |A_j|^2, \quad (2) \\
&\frac{\partial A_3}{\partial z} + \left(\frac{1}{u_3} - \frac{1}{u_1}\right)\frac{\partial A_3}{\partial \eta} - \mathrm{i}\frac{k_{23}}{2}\frac{\partial^2 A_3}{\partial \eta^2} \\
&\quad = -\mathrm{i}\beta A_1^2 e^{\mathrm{i}\Delta kz} - \mathrm{i}A_3 \sum_{j=1}^{3} \gamma_{3,j} |A_j|^2.
\end{aligned}$$

Here, A_1 and A_2 are the field envelopes of the fundamental wave; A_3 is the second-harmonic wave field; β and $\gamma_{i,j}$ are the nonlinear coupling coefficients for the second- and third-order waves; u_j (j = 1, 2, 3) are the group velocities; and $k_{2j} = \partial^2 k_j/\partial\omega^2$. In equations (2), the nonsynchronous generation of second harmonic by wave 2 with envelope A_2 is neglected. The initial boundary conditions are:

$$\begin{aligned}
&A_1(z=0,t) = A_{10}\exp[-2\ln 2(t^2/\tau^2)], \\
&A_2(z=0,t) = A_{10}\exp[-2\ln 2(t^2/\tau^2)], \quad (3) \\
&A_3(z=0,t) = 0.
\end{aligned}$$

Here, τ is the half-height intensity pulse duration, and A_{10} is the field amplitude at input to the nonlinear crystal for waves 1 and 2.

System (2) is also applicable for wave propagation in crystal 2 except for that the expressions for waves 1 and 2 swap and the fields of a fundamental wave from output of the first crystal are used as the initial boundary conditions.

We now analyse possibilities of the method on an example of a BBO crystal. Quadratic and cubic coefficients of wave coupling for this crystal are given in [27]. We will assume that at the input of the nonlinear crystal, wave 1 is ordinary one and wave 2 is extraordinary. The phase matching angle in a uniaxial crystal can be found from the formula:

$$\sin\theta_s^2 = \frac{N_o^{-2}(\omega) - N_o^{-2}(2\omega)}{N_e^{-2}(2\omega) - N_o^{-2}(2\omega)}. \quad (4)$$

Here, $N_o(\omega)$ and $N_e(\omega)$ are the principal values of the refractive index ellipsoid. The linear dispersion of the refractive index results in that pulses of the fundamental and second-harmonic waves scatter in time; moreover, the pulses of fundamental wave also recede from each other due to refractive index anisotropy. The time delay between pulses of the fundamental wave can be found from the following considerations. A pulse of fundamental wave 1 runs through the first nonlinear crystal in the time interval $\tau_1 = L_1/u_1(\lambda)$, and the pulse of the fundamental wave 2 – in the time interval $\tau_2 = L_1/[u_2(\lambda, \theta_s + \Delta\theta_1)]$ ($\Delta\theta_1$ is the angular detuning from the matching position). The time difference $\Delta\tau = |\tau_1 - \tau_2|$ is just the time delay between the pulses of the fundamental waves 1 and 2 in the first crystal (of thickness L_1). Since the pulses of waves 1 and 2 in the second crystal swap (the ordinary pulse becomes extraordinary and vice versa), those overtake each other. For each propagation direction in the second crystal relative to the optical axis, one can find the thickness $\tilde{L}_2$ at which the pulses will exactly coincide. Thickness of the second crystal L_2 is chosen maximum closely to $\tilde{L}_2$ in order to make the difference of linear phases for both fundamental waves at output be multiple of 2π.

Consider the propagation of intense laser pulses with a centre wavelength of 910 nm, duration of 50 fs, and peak intensity of 1.5 TW cm^{-2} in a BBO crystal. Let the far contrast of the pulse be 10^{-7}. We will assume that the shear angle of the first and second crystals in the noncritical plane φ is equal to –90°, and the angles in the critical interaction plane are parameters. The phase-matching angle with respect to the optical axis is 25.9°. For these parameters of laser pulses, the maximal peak intensity of the pulse reflected from the polariser is attained at the crystal thicknesses L_1 = 700 μm and L_2 = 138 μm and at the angular deviations from the matching direction $\Delta\theta_1 = -2.26°$, $\Delta\theta_2 = 64°$. In the second crystal, the radiation propagates at the angle of 90° with respect to the optical axis. Pulse profiles of the fundamental and second-harmonic waves, nonlinear phases, and their

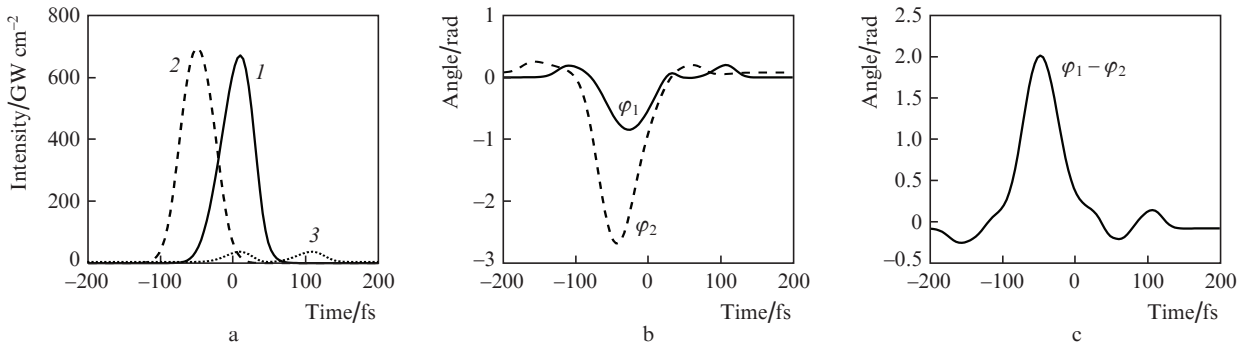

Figure 7. (a) Pulse profiles for (*1*, *2*) the fundamental and (*3*) second-harmonic waves, (b) phases of the fundamental wave pulses, φ_1 and φ_2, and (c) their difference $\Delta\varphi = \varphi_1 - \varphi_2$ at the output from the first BBO crystal of thickness 700 μm.

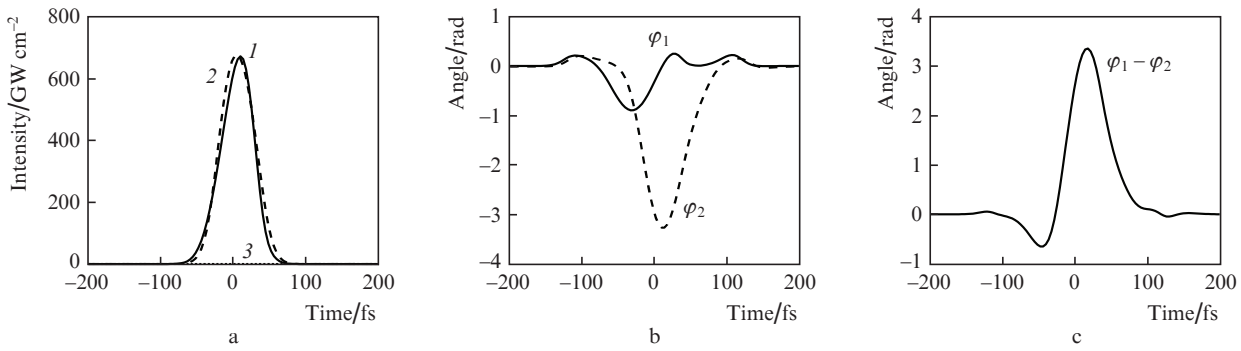

Figure 8. The same as in Fig. 7 at the output from the second BBO crystal of thickness 138 μm.

difference at output of the first crystal are presented in Fig. 7, and for the second crystal in Fig. 8.

At the output from the second crystal, the pulses completely coincide in time, and the phase difference in the pulse statistical centres is close to π. Figure 9 shows the pulse profiles before and after enhancing the contrast by the scheme with two crystals and a polariser 9. The pulse with the enhanced contrast exhibits negligible distortions of the intensity time profile, which are related to the joint manifestation of linear (group recession and dispersion spreading of the pulses) and nonlinear effects. A duration of the pulse with the enhanced contrast reduces to 35 fs.

The peak intensity of the pulse with the enhanced contrast reduced by 11% from the initial value, the pulse duration in this case shortened from 50 fs to 35 fs. The employment of chirped mirrors for spectrum phase correction reduces the duration of the pulse with enhanced contrast to 23 fs and increases its peak intensity by a factor of 1.2 as compared to the intensity of the initial pulse at input of the first nonlinear crystal (see Fig. 9). Note also that a variation of the input intensity by 10% with other parameters (crystal thicknesses and angles of detuning from the phase matching direction) being the same results in only 3% fall in the peak intensity for the pulse with enhanced contrast. The degree of contrast enhancement does not change in this case.

Thus, according to the results of the numerical simulation, the suggested scheme with two uniaxial crystals makes it possible to increase the contrast of the pulse of the fundamental wave by a factor of approximately five orders in magnitude.

4. Conclusions

In the present work, two nonlinear-optical methods are suggested and analysed, which can increase the contrast of laser pulses. The first method based on a nonlinear Mach–Zehnder interferometer will noticeably increase the far contrast if the optical quality of optical elements is high. However, the efficiency of the method falls if the surfaces of interferometer optical elements are produced with an accuracy worse than $\lambda/10$. The second method based on the employment of cascade quadratic nonlinearity in two tandem uniaxial crystals detuned from the matching direction makes it possible to enhance the far contrast by a few orders in magnitude. Both the methods negligibly (~10%) reduce the peak pulse intensity. The employment of spectrum phase correctors at output of the devices described may not only compensate a reduction of the peak intensity relative to that of the initial pulse, but also exceed the latter due to a shorter pulse duration.

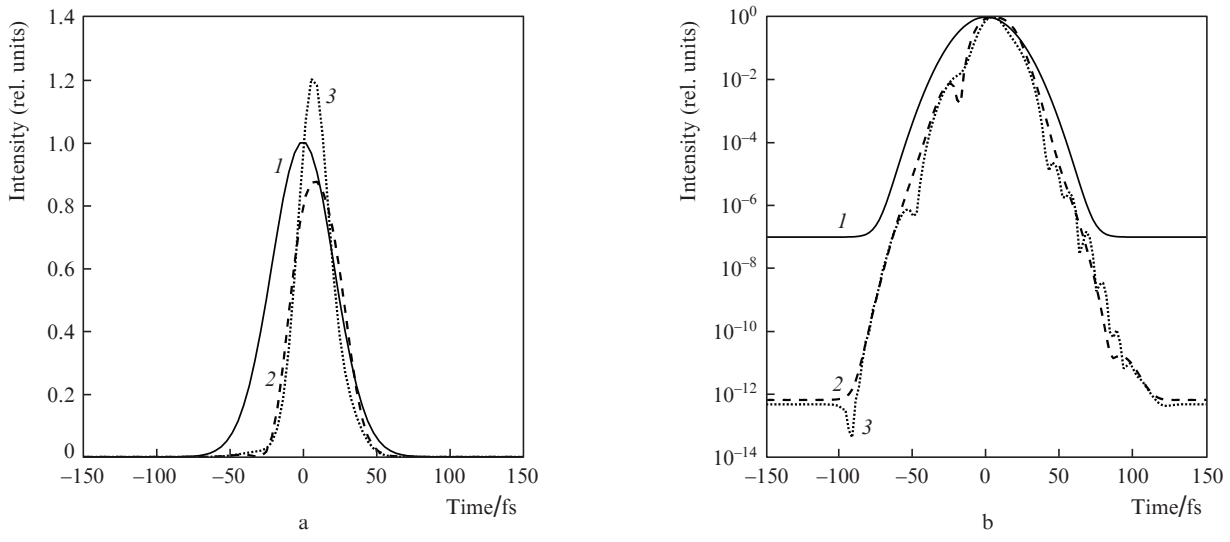

Figure 9. Profiles of pulses: (*1*) initial, (*2*) after enhancing the contrast, and (*3*) after additional time compression in the (a) linear and (b) logarithmic scales.

Acknowledgements. The work was supported by the Ministry of Education and Science of Russian Federation in the frameworks of the FCP project "Investigations and development in priority directions of the scientific-technological complex of Russia in 2014–2020" (Unique Project Identifier RFMEFI6017X0196) and by the Presidium of the Russian Academy of Sciences (Fundamental Research Programme No. 6 "Extreme Light Fields and Their Interaction with Matter").

References

1. Bahk S.W., Rousseau P., Planchon T.A., Chvykov V., Kalintchenko G., Maksimchuk A., Mourou G.A., Yanovsky V. *Appl. Phys. B,* **80**, 823 (2005).
2. Mironov S.Y., Lozhkarev V.V., Ginzburg V.N., Khazanov E.A. *Appl. Opt*., **48**, 2051 (2009).
3. Mironov S.Yu., Lozhkarev V.V., Khazanov E.A., Mourou G.A. *Quantum Electron*., **43**, 711 (2013) [*Kvantovaya Elektron*., **43**, 711 (2013)].
4. Mironov S., Lassonde P., Kieffer J.C., Khazanov E., Mourou G. *Eur. Phys. J. Spec. Top*., **223**, 1175 (2014).
5. Mourou G., Mironov S., Khazanov E., Sergeev A. *Eur. Phys. J. Spec. Top*., **223**, 1181 (2014).
6. Mironov S.Yu., Ginzburg V.N., Yakovlev I.V., Kochetkov A.A., Shaikin A.A., Khazanov E.A., Mourou G.A. *Quantum Electron*., **47**, 614 (2017) [*Kvantovaya Elektron*., **47**, 614 (2017)].
7. Lassonde P., Mironov S., Fourmaux S., Payeur S., Khazanov E., Sergeev A., Kieffer J.C., Mourou G. *Laser Phys. Lett*., **13**, 075401 (2016).
8. Arikawa Y., Kojima S., Morace A., Sakata S., Gawa T., Taguchi Y., Abe Y., Zhang Z., Vaisseau X., Lee S.H., Matsuo K., Tosaki S., Hata M., Kawabata K., Kawakami Y., Ishida M., Tsuji K., Matsuo S., Morio N., Kawasaki T., Tokita S., Nakata Y., Jitsuno T., Miyanaga N., Kawanaka J., Nagatomo H., Yogo A., Nakai M., Nishimura H., Shiraga H., Fujioka S., Group F., Group L., Azechi H., Sunahara A., Johzaki T., Ozaki T., Sakagami H., Sagisaka A., Ogura K., Pirozhkov A.S., Nishikino M., Kondo K., Inoue S., Teramoto K., Hashida M., Sakabe S. *Appl. Opt*., **55**, 6850 (2016).
9. Lévy A., Ceccotti T., D'Oliveira P., Réau F., Perdrix M., Quéré F., Monot P., Bougeard M., Lagadec H., Martin P., Geindre J.-P., Audebert P. *Opt. Lett*., **32**, 310 (2007).
10. Inoue S., Maeda K., Tokita S., Mori K., Teramoto K., Hashida M., Sakabe S. *Appl. Opt*., **55**, 5647 (2016).
11. Jullien A., Albert O., Burgy F., Hamoniaux G., Rousseau J.-P., Chambaret J.-P., Augé-Rochereau F., Chériaux G., Etchepare J., Minkovski N., Saltiel S.M. *Opt. Lett*., **30**, 920 (2005).
12. Stolen R.H., Botineau J., Ashkin A. *Opt. Lett*., **7**, 512 (1982).
13. Kalashnikov M.P., Osvay K., Schönnagel H., Volkov R., Sandner W. *Proc. of CLEO: 2011 – Laser Science to Photonic Applications* (OSA, 2011) Paper CWG3.
14. Chien C.Y., Korn G., Coe J.S., Squier J., Mourou G., Craxton R.S. *Opt. Lett*., **20**, 353 (1995).
15. Ditmire T., Rubenchik A.M., Eimerl D., Perry M.D. *J. Opt. Soc. Am. B*, **13**, 649 (1996).
16. Mironov S.Y., Lozhkarev V.V., Ginzburg V.N., Yakovlev I.V., Luchinin G., Shaykin A., Khazanov E.A., Babin A., Novikov E., Fadeev S., Sergeev A.M., Mourou G.A. *IEEE J. Sel. Top. Quantum Electron*., **18**, 7 (2012).
17. Jullien A., Rousseau J.-P., Mercier B., Antonucci L., Albert O., Chériaux G., Kourtev S., Minkovski N., Saltiel S.M. *Opt. Lett*., **33**, 2353 (2008).
18. Aitchison J.S. et al. *Electron. Lett*., **27**, 1709 (1991).
19. AI-Hemyan K. et al. *Electron. Lett*., **28**, 1090 (1992).
20. Ironside C.N., Aitchison J.S., Arnold J.M. *IEEE J. Quantum Electron*., **29**, 2650 (1993).
21. Saltiel S., Koynov K., Buchvarov I. *Appl. Phys. B*, **63**, 371 (1996).
22. Mironov S., Khazanov E., Mourou G. *Proc. of Advanced Photonics* (Barcelona, 2014) paper JTu3A.24.
23. DeSalvo R., Hagan D.J., Sheik-Bahae M., Stegeman G., Van Stryland E.W., Vanherzeele H. *Opt. Lett*., **17**, 28 (1992).
24. Stegeman G.I., Hagan D.J., Torner L. *Opt. Quantum Electron*., **28**, 1691 (1996).
25. Liu X., Qian L., Wise F. *Opt. Lett*., **24**, 1777 (1999).
26. Beckwitt K., Wise F.W., Qian L., Walker L.A., Canto-Said E. *Opt. Lett*., **26**, 1696 (2001).
27. Bache M., Guo H., Zhou B., Zeng X. *Opt. Mater. Express*, **3**, 357 (2013).